

Study on the boson peak in bulk metallic glasses

Yong Li, Peng Yu, and H. Y. Bai^{a)}

Institute of Physics, Chinese Academy of Sciences, Beijing 100080, People's Republic of China

(Received 2 January 2008; accepted 22 April 2008; published online 10 July 2008)

The low-temperature specific heat (low- T C_p) and other properties of a series of representative bulk metallic glasses (BMGs) were studied. The pronounced low- T C_p anomalies associated with the boson peak (BP) in the representative BMGs were observed. The BMG samples were annealed and quenched near the glass transition temperatures, and the effect of isothermal annealing for different times and quenching at different cooling rates on the low- T C_p anomalies were studied. We observed that the BP is affected by annealing and quenching processes. It is a possible explanation that the BP mainly originated from the random dense cluster-packing structure. The origin of the C_p anomalies is interpreted with the harmonic localized modes based on the random dense-packed atomic cluster structure of BMGs. The clear correlation between the maximum value of BP $[(C_p - \gamma T)/T^3]_{\max}$ and its position T_{\max} further supports the model. © 2008 American Institute of Physics. [DOI: 10.1063/1.2948926]

Although in a glass there is no long-range order over the very long time scales of its structural relaxations, it essentially behaves like a solid with particles oscillating around the mean positions. The low-temperature ($T < 1$ K) vibrational spectra of most glasses are known to deviate from the standard Debye density of states¹ and can be explained quite adequately within the two-level system (TLS).^{2,3} The most intriguing universal feature observed in glasses and undercooled liquids in the Raman or inelastic neutron scattering at low frequencies, which is distinct from the quasielastic peak, is usually referred to as the boson peak (BP).^{4,5} Studies by Raman and other techniques usually cannot separate the contributions from the atomic vibrational density of states $g(\nu)$ and the photon-vibration coupling constant $C(\nu)$. Low-temperature specific heat (low- T C_p) measurements, however, give the $g(\nu)$ without unknown coupling constants. At low- T , the C_p of glasses often presents the distinct excess in C_p/T^3 compared to the Debye theory above 1 K, which is related to the BP contribution. Moreover, the maximum in C_p/T^3 is associated with an excess in the vibrational density of states $g(\nu)/\nu^2$ over Debye behavior. Similarly, the thermal conductivity increases as T^2 with increasing T and exhibits a plateau.

The nature of BP has been one of the debated subjects of condensed-matter physics.^{6–12} Interest in this issue is further stimulated by the finding of the relationship between the amplitude of BP and the properties such as liquid fragility m , defined as the change in viscosity η with T approaching glass transition temperature T_g (Ref. 13) in nonmetallic glasses.^{14,15} However, the origin of BP is still a debated issue. It is unclear as to how generally such anomaly might be in various glasses and how it relates to the features of glasses. Furthermore, previous studies on BP are mainly concentrated on network or polymeric glasses. The nature of BP might be difficult to be well understood only by investigating the mo-

lecular glasses because the intramolecular, reorientational, and translational motions of molecules in these glasses all may contribute to BP. Metallic glass with a simple atomic glassy structure (without reorientation and intramolecular processes) could provide clearer evidence for the underlying physics of BP. Recently, a series of new bulk metallic glasses (BMGs) with excellent glass-forming ability, configurational features, and unique properties has been developed.^{16,17} Particularly, the BMGs cover the main part of the Angell diagram in terms of fragility¹³ and show specific-heat anomaly.^{18,19} The availability of such glasses with a close packed Bernal structure,²⁰ which are markedly different from nonmetallic glasses, makes it possible to study systematically the low- T C_p anomaly associated with the generation of low-frequency modes. BMGs differ from the traditional rapidly quenched metallic glasses in the fact that a significantly slower cooling rate is required to get bulk glassy alloys.¹⁶ This usually leads to the formation of locally favored structures and atomic clusters in undercooled alloy melts during cooling.²¹ As a result, the low- T C_p of metallic glass may not be described by the Debye model only and additional vibrational modes, which are related with their unique structures, might exist. However, up to now, little work on BP is reported in the metallic glassy materials.^{18,19}

The effect of thermal history on BP is also unclear.^{22,23} It is well known that the physical properties of a glass and thus the nature of atomic packing is a function of thermokinetic history. Fast quenching affects local atomic structure, density, and sound velocity, therefore, influences the vibrational dynamics and BP via the macroscopic parameters. The dependence of BP on both cooling rate and the relaxation is the subject of active research efforts.^{24–28} New progress in this topic has been achieved in the concept of “energy landscape.”^{29–32} However, the change in the BP in the BMGs after annealing or quenching treatment has not been investigated. The lack of information impedes the understanding of BP. The structural relaxation kinetics of metallic glass has been explained by free-volume theory, which was formulated

^{a)}Author to whom correspondence should be addressed. Electronic mail: hybai@aphy.iphy.ac.cn.

TABLE I. The fitting coefficients (γ and β) from the least-squares linear fit of $C_p/T = \gamma + \beta T^2$ in the low-temperature part (≤ 8 K), the Debye temperature θ_D , the BP amplitude $[(C_p - \gamma T)/T^3]_{\max}$ and the position T_{\max} in the high-temperature region for our measured representative BMGs. The constant magnetic-cluster contribution A to C_p for $(\text{Cu}_{50}\text{Zr}_{50})_{90}\text{Al}_7\text{Gd}_3$ BMG and the fragilities m determined thermodynamically for our measured BMGs are also listed.

	Fitting results from low- T part (< 8 K)			θ_D (K)	T_{\max} (K)	$[(C_p - \gamma T)/T^3]_{\max}$ (mJ/mol K ⁴)	Fragility m
	A (J/mol K)	γ (mJ/mol K ²)	β (mJ/mol K ⁴)				
$\text{Cu}_{50}\text{Zr}_{50}$...	4.3	0.1	270	16.4	0.123	62
$(\text{Cu}_{50}\text{Zr}_{50})_{96}\text{Al}_4$...	3.46	0.16	268	10.3	0.178	40
$(\text{Cu}_{50}\text{Zr}_{50})_{92}\text{Al}_8$...	3.06	0.17	298	12.6	0.146	43
$\text{Pd}_{40}\text{Ni}_{40}\text{P}_{20}$...	2.19	0.16	288	9.9	0.18	46 ^a
vit4	...	3.36	0.11	310	11.6	0.123	43 ^a
$\text{Pd}_{40}\text{Ni}_{10}\text{Cu}_{30}\text{P}_{20}$...	0.73	0.16	280	10.7	0.185	57 ^a
$(\text{Cu}_{50}\text{Zr}_{50})_{90}\text{Al}_7\text{Gd}_3$	0.099 82	4.77	0.21	260	7.23	0.207	30

^aReference 52, and references therein.

by Cohen and Turnbull.³³ Structural relaxation during annealing or lower cooling rate quenching corresponds to the annihilation of the excess free volume. With increasing annealing time, the excess free volume decreases approaching to the equilibrium.³⁴ The production or annihilation of the free volume should also have influence on the BP. Recently, the discovered BMGs enable us to promote the study of structural relaxation influence on the BP in a sub- T_g region because of their high resistance to crystallization.¹⁶

In this work, we report the pronounced low- T C_p anomalies in a series of BMGs, and their dependence on annealing times and quenching rates. One of the aims of this work is to investigate the effect of thermal history, particularly the effect of annealing and quenching on BP. The data coming from the low- T C_p measurements are expected to provide experimental evidence and points of view on the nature and the atomic packing in disordered matter, particularly in BMGs. The $(\text{Cu}_{50}\text{Zr}_{50})_{92}\text{Al}_8$ BMG samples were isothermally annealed below the glass transition temperature and the $\text{Zr}_{46.75}\text{Ti}_{8.25}\text{Cu}_{7.5}\text{Ni}_{10}\text{Be}_{27.5}$ (Vit4) BMG samples were quenched at different cooling rates. The effect of isothermal annealing for different times and quenching at different cooling rates on the low- T C_p anomalies were studied. We found that the change in the magnitudes of the BP in these BMGs mainly comes from the annealing or the quenching treatments other than the Debye one. We also found that the C_p anomalies can be attributed to the harmonic localized Einstein modes in the simple atomic glasses with a disordered dense-packed atom cluster structure. The clear correlation between the maximum of BP $[(C_p - \gamma T)/T^3]_{\max}$ and its position T_{\max} further supports the model.

A series of representative BMGs (listed in Table I) with markedly different properties are chosen as the model glasses to study the low- T C_p . For the preparation of the BMGs, readers are referred to Ref. 16. For the C_p measurements, the square-shaped plates with a size of $3 \times 2 \times 1$ mm³ were used. C_p was measured by Physical Property Measurement System using PPMS 6000 with an accuracy of about 2%. The fragility m of the BMGs was determined thermodynamically, which was confirmed by previous studies equally well as the complementary viscosity measurements.³⁵ The temperature range of the C_p measurement is from 2 to 50 K or

higher. To analyze the C_p data, one needs to determine the electronic contribution and/or constant magnetic-cluster contribution correctly using the method that was previously reported.^{18,19} The fitting coefficients of the electronic coefficient γ and constant contribution A for all of the studied BMGs are compiled in Table I.

Figure 1 shows the $(C_p - \gamma T)/T^3$ without the mask of the electronic and/or magnetic contributions. The results clearly exceed the Debye model and show an anomaly. The fragile glasses show hardly pronounced bump, which is general for other fragile nonmetallic glasses.^{14,15} The bump becomes more pronounced, and the T_{\max} shifts to lower T for the stronger BMGs. As in many nonmetallic glasses, it is reasonable to believe that the humps arise from the excess low-frequency vibrations and correspond to the BP.^{4,5,14}

The value of the maximum $[(C_p - \gamma T)/T^3]_{\max}$, increases with the decreasing m , i.e., the excess C_p becomes much larger in the stronger BMGs. The values of $(C_p/T^3)_{\max}$ of the oxide and organic glasses are 10–20 times larger than those of BMGs because of the large Debye contribution to C_p in those nonmetallic glasses.^{14,36–38} C_{BP} is obtained from subtracting the Debye contribution γT and/or the magnetic contribution A from the measured C_p : $C_{\text{BP}}/C_D = (C_p - C_D - \gamma T)$

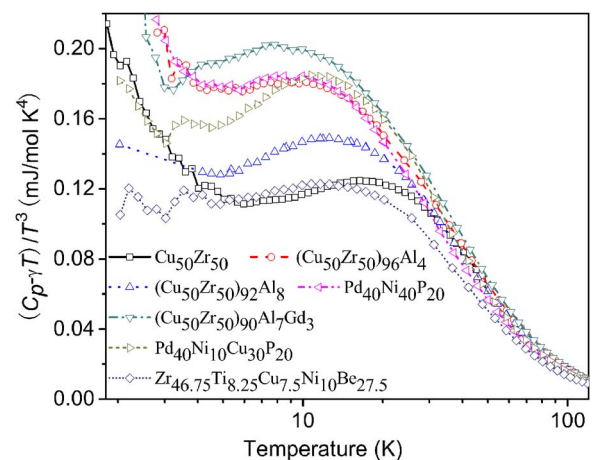


FIG. 1. (Color online) The $(C_p - \gamma T)/T^3$ vs T plots of our measured representative BMGs after subtracting the electronic and/or magnetic contributions.

TABLE II. The amplitude of the BP in the different forms $[(C_p - \gamma T)/T^3]_{\max}$ and $(C_{BP}/C_D)_{\max}$, their positions T_{\max} , and the fragilities m for our measured BMGs and some traditional glasses collected from literatures used in comparing the fragility and the maximum values of BP $(C_{BP}/C_D)_{\max}$, or in the relation between the maximum values of BP $[(C_p - \gamma T)/T^3]_{\max}$ and its position T_{\max} .

	T_{\max} (K)	$[(C_p - \gamma T)/T^3]_{\max}$ $\mu\text{J/g K}^4$	$(C_{BP}/C_D)_{\max}$	Fragility m
Our measured results for BMGs				
$\text{Cu}_{50}\text{Zr}_{50}$	16.4	1.59	0.246	62
$(\text{Cu}_{50}\text{Zr}_{50})_{96}\text{Al}_4$	10.3	2.36	0.761	40
$(\text{Cu}_{50}\text{Zr}_{50})_{92}\text{Al}_8$	12.6	1.99	0.745	43
$\text{Pd}_{40}\text{Ni}_{40}\text{P}_{20}$	9.9	2.49	1.215	46 ^a
Vit4	11.6	2.06	0.88	43 ^a
$\text{Pd}_{40}\text{Ni}_{10}\text{Cu}_{30}\text{P}_{20}$	10.7	2.51	1.09	57 ^a
$(\text{Cu}_{50}\text{Zr}_{50})_{90}\text{Al}_7\text{Gd}_3$	7.23	2.71	0.868	30
$\text{La}_{65}\text{Al}_{10}\text{Cu}_{20}\text{Co}_5$	7.2	9.42	1.586	...
$\text{Tb}_{36}\text{Y}_{20}\text{Al}_{24}\text{Co}_{20}$	7.8	6.29	1.561	...
Data collected from literatures ^b				
SiO_2	10.8	4	4	20
GeO_2	8.4	3	1.5	24
B_2O_3	5	8.1	1.1	44
As_2Se_3	4.7	13.2	1.5	...
As_2S_3	4.9	7.8	1	39
$3\text{SiO}_2\text{-N}_2\text{O}$	13.5	2.3	2.1	...
Se	3.4	17.9	1.1	71
Glycerol	7	7.2	0.75	48
Polybutadiene (PB)	5.1	15.8	0.64	...
<i>o</i> -terphenyl (OTP)	2.2	20.8	0.56	82
CKN	6	3.1	0.4	93
As	5	7.4
Lexan	2.2	31.5	1.1	...
PS	3	32.5	1.3	...
PMMA	3.6	15	0.82	...
PET	3.5	12.5	5	...
Ethanol	5	24
$(\text{Na}_2\text{O})_{20}(\text{SiO}_2)_{80}$	1.3	37

^aReference 52.

^bReference 53.

$-A)/C_D$. After scaled by C_D , the effect of varying the Debye contribution, which is usually the major part in C_p , is eliminated. The values of C_{BP}/C_D in the BMGs, oxide glasses, and organic glasses obey a correlation between the BP and m only with an exception of SiO_2 (Ref. 39) (data have also been listed in Table II). Figure 2, even more points for our measured representative BMGs are included, shows the relationship between C_{BP}/C_D and m that is identical to that advanced by Sokolov.^{14,15}

Glass is formed from cooling a highly viscous liquid out of the equilibrium.⁴⁰⁻⁴² Obviously, the liquid atom or molecular arrangement at the transition temperature has a determining influence on the properties of the solid such as density and short-range order. In the free-volume theory, the structural change is described intuitively as a gradual reduction in the free volume.³³ It has been found that the calorimetric glass transition is accompanied by the production of the free volume.⁴³ Structural relaxation, which occurs during isothermal annealing, corresponds to the annihilation of the excess free volume. The BMGs are expected to be ideal glassy system for investigating the influence of the free vol-

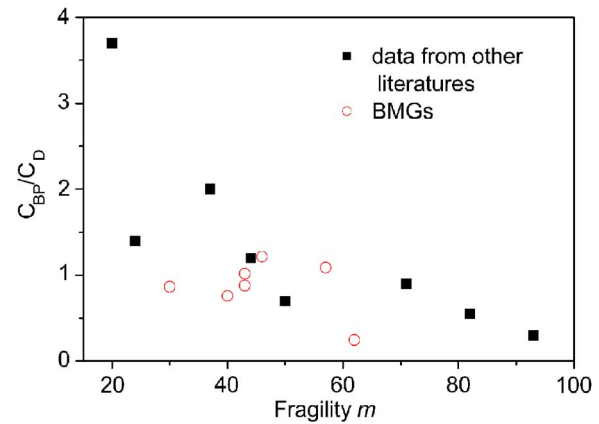


FIG. 2. (Color online) The ratio of the BP to the Debye contributions around the maximum vs the fragility m of our measured BMGs and some traditional glasses collected from literatures. The data are also listed in Table II.

ume on the low- T C_p since they are comparable well to a hard-sphere system and possess higher thermal stability. In order to investigate the effects of the annealing process on the low- T C_p anomaly, the annealing of the as-cast $(\text{Cu}_{50}\text{Zr}_{50})_{92}\text{Al}_8$ BMG sample was performed at 673 K below the calorimetric glass transition temperature (701 K) for different times in a furnace with a vacuum of 2.0×10^{-3} Pa. The stability of the temperature is controlled within ± 1 K. The samples were annealed for 1, 4, and 20 h, respectively. Figure 3(a) shows the $(C_p - \gamma T)/T^3$ of the as-cast and annealed $(\text{Cu}_{50}\text{Zr}_{50})_{92}\text{Al}_8$ BMGs without the mask of the electronic contributions. All the fitting coefficients are listed in Table III. Figure 3(a) demonstrates clearly the annealing effect on the low- T C_p . At about 14 K, the height of peak in C_p decreases during the annealing process. It had been pointed out that the excess free volume in the BMG system decreases with the increasing annealing time.⁴³ So the reduced peak height of the low- T C_p should be relative to the decreasing excess free volume. However, it cannot be confirmed that the change in the peak comes only from the decreasing excess free volume. It can also come from the change in the Debye term, i.e., it can often be compensated by a corresponding increase in the Debye one. The Debye temperature was calculated from the fitting of the high-temperature part of C_p for the as-cast and the annealed $(\text{Cu}_{50}\text{Zr}_{50})_{92}\text{Al}_8$ BMGs. The results are also compiled in Table III. With the varying of the annealing time, the Debye temperature changes also. In order to evaluate the effect of the annealing time, the low-temperature peaks were rescaled by the Debye term using the fitting results and were renormalized. In Fig. 3(a), there is no evident difference between the peaks after the different annealing processes. However, after subtracting the Debye contributions, the peaks change their dependence manner on the annealing time [see Fig. 3(b)]. This implies that annealing affects both the Debye contribution and the BP. Therefore, the continuous medium of the BMGs has also transformed after annealing. Coupled with the transformation of the elastic medium of the BMGs, the Debye term changes inevitably. Subtracting the influence of the changed Debye term, the dependence of the BP on the annealing time was unmasked [Fig. 3(b)]. From Fig. 3(b), it can be seen that the amplitude

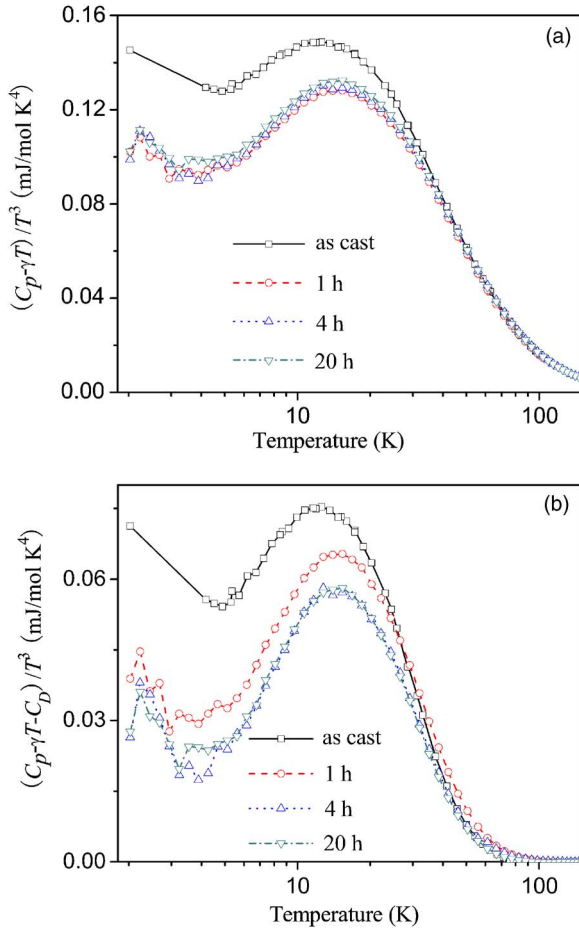


FIG. 3. (Color online) The $(C_p - \gamma T)/T^3$ (a) and $(C_p - \gamma T - C_D)/T^3$ (b) vs T plots of the as-cast and annealed $(\text{Cu}_{50}\text{Zr}_{50})_{92}\text{Al}_8$ BMGs. The annealing of $(\text{Cu}_{50}\text{Zr}_{50})_{92}\text{Al}_8$ BMGs was performed at 673 K below the calorimetric glass transition temperature (701 K) for 1, 4, and 20 h.

of the BP decreases upon the annealing times, while T_{\max} shifts to the higher temperatures. No obvious change occurred in the sample annealed for 20 h since the relaxation process has approached to the limit.

TABLE III. The fitting coefficients (γ and β) from the least-square linear fit of $C_p/T = \gamma + \beta T^2$ in the low-temperature part (≤ 8 K), the Debye temperature θ_D , the BP amplitude at different forms $[(C_p - \gamma T)/T^3]_{\max}$ and $[(C_p - \gamma T - C_D)/T^3]_{\max}$, and position T_{\max} , in the high-temperature region for the as-cast and annealed $(\text{Cu}_{50}\text{Zr}_{50})_{92}\text{Al}_8$ and the quenched $\text{Zr}_{46.75}\text{Ti}_{8.25}\text{Cu}_{7.5}\text{Ni}_{10}\text{Be}_{27.5}$ (Vit4) BMGs. The annealing of $(\text{Cu}_{50}\text{Zr}_{50})_{92}\text{Al}_8$ BMGs was performed at 673 K below the calorimetric glass transition temperature (701 K) for 1, 4, and 20 h. The quenching of the as-cast Vit4 BMG involved the heating up to 713 K at a heating rate of 40 K/min and the cooling down to room temperature at cooling rates of 160 and 40 K/min.

Treatments	Fitting results from low- T part (< 8 K)					
	γ (mJ/mol K ²)	β (mJ/mol K ⁴)	θ_D (K)	T_{\max} (K)	$[(C_p - \gamma T)/T^3]_{\max}$ (mJ/mol K ⁴)	$[(C_p - \gamma T - C_D)/T^3]_{\max}$ (mJ/mol K ⁴)
$(\text{Cu}_{50}\text{Zr}_{50})_{92}\text{Al}_8$						
As cast	3.06	0.17	298	12.6	0.146	0.0754
Annealed for 1 h at 673 K	2.97	0.1	314	15.4	0.128	0.0654
Annealed for 4 h at 673 K	3.12	0.9	300	15.4	0.13	0.0581
Annealed for 20 h at 673 K	3.09	0.1	297	15.4	0.132	0.0582
Vit4						
As cast	3.36	0.11	310	11.6	0.123	0.0574
Cooling rate of 160 K/min from 713 K	3.43	0.1	314	14	0.106	0.0432
Cooling rate of 40 K/min from 713 K	3.47	0.1	308	12.8	0.112	0.0451

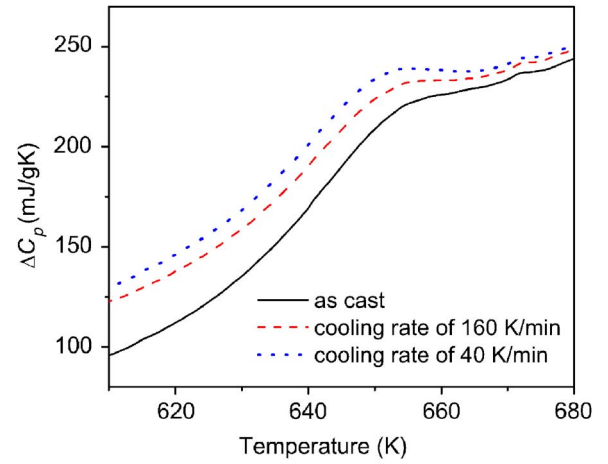


FIG. 4. (Color online) The curves of the DSC obtained from the as-cast and quenched $\text{Zr}_{46.75}\text{Ti}_{8.25}\text{Cu}_{7.5}\text{Ni}_{10}\text{Be}_{27.5}$ (Vit4) BMGs. The quenching process involves the heating up to 713 K at a heating rate of 40 K/min and the cooling down to room temperature at cooling rates of 160 and 40 K/min, respectively.

In order to affirm the investigated annealing effect on both the Debye term and the BP, the quenching of the as-cast $\text{Zr}_{46.75}\text{Ti}_{8.25}\text{Cu}_{7.5}\text{Ni}_{10}\text{Be}_{27.5}$ (Vit4) BMG is performed in PerkinElmer DSC7 with different cooling rates. The process involved the heating up to 713 K at a heating rate of 40 K/min and cooled down to room temperature at the cooling rates of 160 and 40 K/min, respectively. Figure 4 shows the differential scanning calorimetry (DSC) curves of the as-cast Vit4 and two quenched samples at different cooling rates. No crystallization occurred examined by the DSC during the heating process. It is found that the height of the glass transition peak is increased by the lower rate quenching, which is consistent with the other reports.⁴³ This means that the excess free volume in the system decreases with the decreasing cooling rate. When reheating the glass quenched at lower cooling rate by DSC, the relaxed glass absorbs more energy to recover the free volume in order to attain equilibrium and

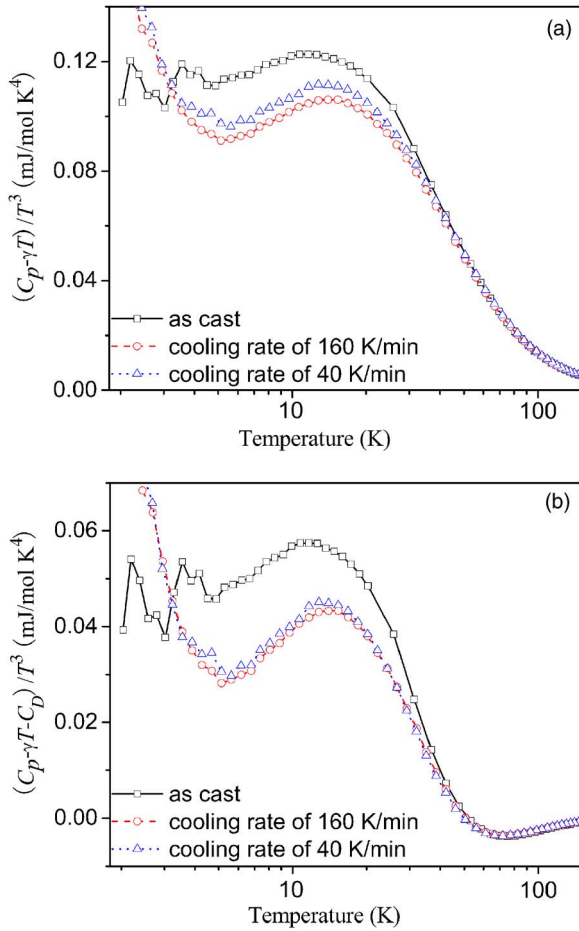


FIG. 5. (Color online) The $(C_p - \gamma T) / T^3$ (a) and $(C_p - \gamma T - C_D) / T^3$ (b) vs T plots of the as-cast and quenched vit4 BMGs. The quenching process involves the heating up to 713 K at a heating rate of 40 K/min and the cooling down to room temperature at cooling rates of 160 and 40 K/min, respectively.

exhibits the overshoots, as shown in Fig. 4. Figure 5(a) shows the $(C_p - \gamma T) / T^3$ of the as-cast and quenched Vit4 BMGs without the mask of the electronic contribution. All the fitting coefficients are listed in Table III. Figure 5(a) demonstrates clearly the quenching effect on the low- T C_p . At about 13 K, the peak height of the low- T C_p decreases by the quenching process. The Debye temperature was fitted from the high-temperature part of C_p for the as-cast and quenched Vit4 BMGs. The results are also compiled in Table III. We note that in Fig. 5 and Table III, one can see that the BP is slightly higher and shifted a little to lower temperatures in the sample with the lower cooling rate (40 K/min) in comparison with the sample with the higher cooling rate (160 K/min). This is in contradiction with our conclusion that the sample with high fraction of free volume has higher BP. We indicate that this resulted from the measurements accuracy. Actually, the cooling rate difference (40 and 160 K/min) does not induce such large difference that could be distinguished by specific heat measurement (DSC has much better accuracy compared with specific heat measurements in our experiments). We note that with the varying of the cooling rates, the Debye temperature also changes. When the low-temperature peaks were rescaled by the Debye term using the fitted results and renormalized, as shown in Fig. 5(b), one

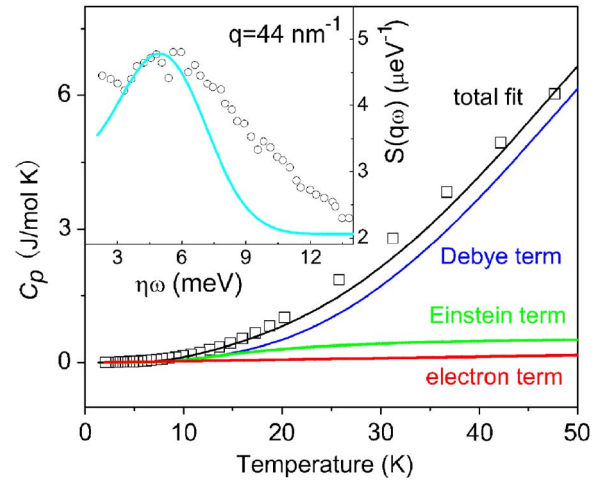


FIG. 6. (Color online) The fitting results (solid lines) including the contributions of the Debye mode and the Einstein mode of the C_p of vit4 BMG between 2 and 50 K. The inset shows the derived VDOS of Vit4 from the C_p (solid line) and neutron inelastic scattering (circles) (Ref. 47). The Vit4 has an Einstein mode with $\theta_E = 57$ K. The agreement rather supports the picture in which the BP in the metallic glasses is ascribed to the localized vibration modes.

can see that the discrepancy of the two samples becomes much smaller, and both gives out almost the same result as in the annealed $(\text{Cu}_{50}\text{Zr}_{50})_{92}\text{Al}_8$ BMG.

After annealing and quenching treatments, the continuous medium of the BMGs transforms. The Debye contribution to C_p changes inevitably. Subtracting the influence of the changing Debye contribution, the dependence of the BP on the annealing times and quenching rates was unmasked. Although we cannot obtain the conclusion that the lowered magnitudes of the BP are directly derived from the annealing process or low rate quenching, we indeed can get out a similar result from Figs. 3 and 5. Thus, the observed effect of the annealing and quenching in C_p comes from the changes in both the BP and the Debye contributions.

The C_p of an elastic continuum normally can be explained by the Debye model in a wide temperature range. However, C_p of these BMGs in the large temperature range cannot be well fitted only by the Debye and the electron contributions. We found that an additional Einstein mode is required to fit C_p adequately. This is illustrated in Fig. 6 for Vit4 BMG. The solid line in Fig. 6 represents a fit: $C_p = \gamma T + C_D + n_E C_E$, where C_D represents the Debye term with $\theta_D = 310$ K, C_E is the Einstein term: $C_E = R(\theta_E/T)^2 e^{\theta_E/T} / (e^{\theta_E/T} - 1)^2$, with an Einstein temperature $\theta_E = 57$ K, and the Einstein oscillator strength per mole $n_E = 0.023$. We also find that the existence of the Einstein oscillators is ubiquitous for a variety of BMGs available. It has been known that localized harmonic vibration modes may exist in the traditional glass.⁴⁴ Therefore, these localized vibration modes will naturally result in an additional Einstein-type vibration, i.e., localized harmonic vibration with a specific frequency. The vibration density of states (VDOS) can be derived from C_p .^{45,46} The derived total VDOS of the Vit4 in the units of oscillators per mole is shown in the inset of Fig. 6. Clearly, the Einstein mode induces a peak below 10 meV. The experimental VDOS from neutron inelastic scattering⁴⁷ of Vit4 was

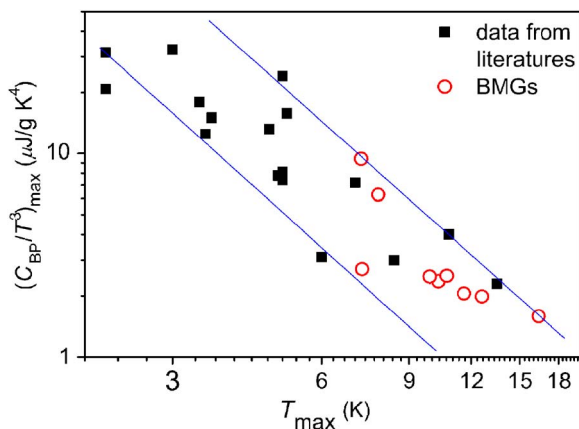


FIG. 7. (Color online) The relation between the maximum values of BP $[(C_p - \gamma T)/T^3]_{\max}$ and its position T_{\max} of our measured BMGs and some traditional glasses collected from literatures. The data are also listed in Table II.

also showed in Fig. 6. In Vit4, the peak at 4.9 meV induced by the Einstein oscillator in the derived VDOS from C_p has almost the same energy and similar shape as the BP (about 5 meV) determined by neutron scattering.⁴⁷ The agreement between neutron scattering result and the VDOS derived from C_p supports a picture in which the BP in the metallic glasses is ascribed to the localized vibration modes.

A truly localized mode appears as a delta function in the VDOS. However, most of loose atoms located at different cluster interstices are easy to hybridize with other acoustic phonons. Due to the hybridization, the frequency of the localized mode is distributed over a considerable range, and hence, the BP appeared in the low- T C_p presents a broad maximum. Therefore, the contribution of the localized modes to VDOS has a Gaussian distribution deviating from the Debye mode.^{45,46} At high T (>10 meV), the hybridization with other modes is stronger, and the peak is considerably broader; meanwhile, the magnitude of the maximum is decreased. In some cases, the BP is not obvious and cannot be separated from the experimental C_p curve. In fact, the BP at ~ 5.9 meV for $\text{Cu}_{50}\text{Zr}_{50}$ is indeed broader than that of $(\text{Cu}_{50}\text{Zr}_{50})_{96}\text{Al}_4$ (~ 4.9 meV) and $(\text{Cu}_{50}\text{Zr}_{50})_{90}\text{Al}_7\text{Gd}_3$ (~ 4.5 meV) (see Figs. 2 and 5). This result has been summarized in Table II and Fig. 7 with the data collected from the literature for several representative traditional glasses. By plotting $[(C_p - \gamma T)/T^3]_{\max}$ versus T_{\max} , the maximum can be scaled into a universal correlation that implies some universal features in the vibrational density of states $g(\nu)$. Indeed, Raman and inelastic neutron scattering demonstrated that the BP for a variety of amorphous solids has a universal form if scaled by its height and position.⁴⁸ Thus, if a determination of the absolute value of $g(\nu)$ is possible, one might also expect a relation between the height and position of the $g(\nu)/\nu^2$ maximum, similar to that of $[(C_p - \gamma T)/T^3]_{\max}$ and T_{\max} .

The Einstein-type localized vibrational mode was also found in $\text{Ni}_{59.5}\text{Nb}_{33.6}\text{Sn}_{6.9}$ (Ref. 49) and Ca-based⁵⁰ BMG. The localized vibrational mode in $\text{Ni}_{59.5}\text{Nb}_{33.6}\text{Sn}_{6.9}$ BMG has been explained to originate from the polytetrahedral short-range ordering, which causes resonant scattering of phonons at low temperatures and eventually results in the localization

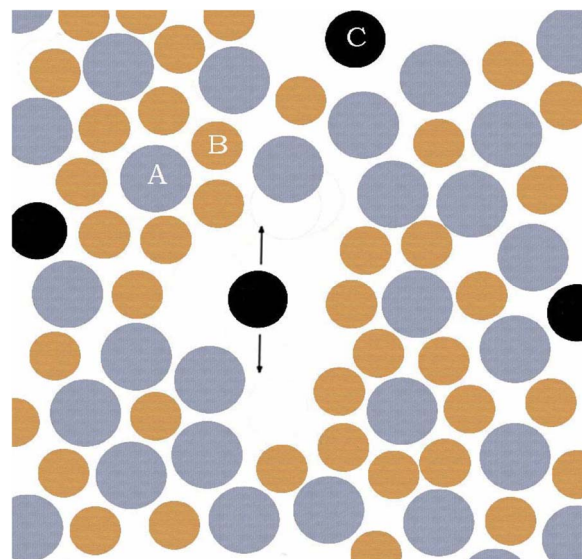


FIG. 8. (Color online) A two dimensional representation of a random dense-packed atom cluster structure for a representative ternary BMG. The gray and brown spheres denote the cluster atoms, and the black spheres denote the loose atoms between the clusters which vibrate with an independently and localized harmonic mode.

of phonons.⁴⁹ The Einstein modes in Ca-based BMG is related to the relatively large size of the Ca ion, which leads to a more open, less dense structure.⁵⁰ The presence of an Einstein oscillator suggests the existence of the vibrations of loose or weak bound atoms or atomic clusters with the independent localized harmonic modes in the glasses. Although the structure of glasses at the nanometric scale is still an open question, some researchers also pointed out that the atomic arrangement is regarded as closely packed domains separated by less ordered zones, thus producing the contrast of elastic constant at the nanometric scale. The random dense cluster-packing model⁵¹ is schematically illustrated in Fig. 8. The spherulike clusters (~ 0.7 – 1.0 nm) are efficiently packed to fill the space, in which there are significant internal strains that prevent the development of long-range order, and defects can also exist within the dense-packed clusters. This model accurately provides richness to the structural description of BMGs and a remarkable ability to predict BMG compositions for various alloys. Some atoms or small atomic clusters, which are independent of others, can play the role of the loose or weak bound particles, vibrating with the localized harmonic modes. The BMGs obtained by rapid quenching from the liquids, to some extent, can inherit liquid structure and contain a large number of nanometer sized clusters and free volumes. The atoms between the clusters or small atom clusters sitting in the sufficiently large free volumes are loosely or weakly bound. They can vibrate in the independent harmonic modes. The assumption is confirmed to some extent in our annealing and quenching results and by Angell,²⁹ who found a much stronger BP in hyperquenched glasses.

In conclusion, the pronounced low- T C_p anomalies associated with the BP in a series of representative BMGs and their dependence on annealing quenching are studied. The BP was observed in all our investigated BMGs. The BP con-

tribution in C_p for the BMGs increases with the decreasing fragility m , i.e., the excess C_p becomes much stronger in the strong BMGs, which is similar to the correlation that advanced by Sokolov.^{14,15} The effect of thermal history on the BP was also investigated. The results show that not only the peak of the glass transition in the DSC curves is affected by the thermal treatments, the peak in low- T C_p is also affected by the annealing and quenching processes. We find that the magnitude of the BP decreases after annealing and quenching at lower cooling rates. An additional Einstein mode is required to fit the C_p results adequately and the BP in the metallic glasses is ascribed to the localized vibration modes. The clear correlation between the maximum values of the BP $[(C_p - \gamma T)/T^3]_{\max}$ and its position T_{\max} further supports to the model. The presence of the Einstein oscillators in the atomic glasses is interpreted with the harmonic localized modes based on the random dense-packed atomic cluster structural model of metallic glass.

The financial support of the NSF of China (Grant Nos. 50671117 and 506210611) is appreciated.

¹*Amorphous Solids: Low-Temperature Properties*, edited by W. A. Phillips (Springer, Berlin, 1981).

²P. W. Anderson, B. I. Halperin, and C. M. Varma, *Philos. Mag.* **25**, 1 (1972).

³W. A. Phillips, *J. Low Temp. Phys.* **7**, 351 (1972).

⁴U. Buchenau, N. Nucker, and A. J. Dianoux, *Phys. Rev. Lett.* **53**, 2316 (1984).

⁵F. Sette, M. H. Krisch, C. Masciovecchio, G. Ruocco, and G. Monaco, *Science* **280**, 1550 (1998).

⁶W. Schirmacher, G. Ruocco, and T. Scopigno, *Phys. Rev. Lett.* **98**, 025501 (2007).

⁷P. Benassi, M. Krisch, C. Masciovecchio, V. Mazzacurati, G. Monaco, G. Ruocco, F. Sette, and R. Verbeni, *Phys. Rev. Lett.* **77**, 3835 (1996).

⁸B. Rufflé, G. Guimbretière, E. Courtens, R. Vacher, and G. Monaco, *Phys. Rev. Lett.* **96**, 045502 (2006).

⁹C. Masciovecchio, G. Baldi, S. Caponi, L. Comez, S. Di Fonzo, D. Fioretto, A. Fontana, A. Gessini, S. C. Santucci, F. Sette, G. Viliani, P. Vilmercati, and G. Ruocco, *Phys. Rev. Lett.* **97**, 035501 (2006).

¹⁰A. Monaco, A. I. Chumakov, Y.-Z. Yue, G. Monaco, L. Comez, D. Fioretto, W. A. Crichton, and R. Ruffer, *Phys. Rev. Lett.* **96**, 205502 (2006).

¹¹A. Monaco, A. I. Chumakov, G. Monaco, W. A. Crichton, A. Meyer, L. Comez, D. Fioretto, J. Korecki, and R. Ruffer, *Phys. Rev. Lett.* **97**, 135501 (2006).

¹²M. Turlakov, *Phys. Rev. Lett.* **93**, 035501 (2004).

¹³R. Bohmer and C. A. Angell, *Phys. Rev. B* **45**, 10091 (1992).

¹⁴A. P. Sokolov, R. Calemczuk, B. Salce, A. Kisliuk, D. Quitmann, and E. Duval, *Phys. Rev. Lett.* **78**, 2405 (1997).

¹⁵V. N. Novikov and A. P. Sokolov, *Nature (London)* **431**, 961 (2004).

¹⁶W. H. Wang, C. Dong, and C. H. Shek, *Mater. Sci. Eng., R.* **44**, 45 (2004);

W. H. Wang, *Prog. Mater. Sci.* **52**, 540 (2007).

¹⁷W. H. Wang, *J. Appl. Phys.* **99**, 093506 (2006); M. B. Tang, D. Q. Zhao, M. X. Pan, and W. H. Wang, *Chin. Phys. Lett.* **21**, 901 (2004).

¹⁸Y. Li, P. Yu, and H. Y. Bai, *Appl. Phys. Lett.* **86**, 231909 (2005).

¹⁹M. B. Tang, H. Y. Bai, and W. H. Wang, *Phys. Rev. B* **72**, 012202 (2005).

²⁰J. D. Bernal, *Nature (London)* **185**, 68 (1960).

²¹H. Tanaka, *J. Non-Cryst. Solids* **351**, 3396 (2005).

²²E. Duval, T. Achibat, A. Boukenter, and A. Mermet, *Philos. Mag. B* **71**, 625 (1995).

²³R. Zorn and B. Frick, *J. Chem. Phys.* **108**, 3327 (1998).

²⁴N. Shimodaira, K. Saito, N. Hiramitsu, S. Matsushita, and A. J. Ikushima, *Phys. Rev. B* **71**, 024209 (2005).

²⁵J. B. Suck, *J. Non-Cryst. Solids* **293–295**, 370 (2001).

²⁶S. Etienne, L. David, A. J. Dianoux, L. Saviot, and E. Duval, *J. Non-Cryst. Solids* **307–310**, 109 (2002).

²⁷E. Duval, L. Saviot, L. David, S. Etienne, and J. F. Jal, *Europhys. Lett.* **63**, 778 (2003).

²⁸N. Shimodaira, K. Saito, N. Hiramitsu, S. Matsushita, and A. J. Ikushima, *Phys. Rev. B* **71**, 024209 (2005).

²⁹C. A. Angell, Y. Yue, L.-M. Wang, J. R. D. Copley, S. Borick, and S. Mossa, *J. Phys.: Condens. Matter* **15**, S1051 (2003).

³⁰C. A. Angell, *J. Phys.: Condens. Matter* **16**, S5153 (2004).

³¹T. S. Grigera, V. Martin-Mayor, G. Parisi, and P. Verrocchio, *Nature (London)* **422**, 289 (2003).

³²G. Parisi, *J. Phys.: Condens. Matter* **15**, S765 (2003).

³³M. H. Cohen and D. Turnbull, *J. Chem. Phys.* **31**, 1164 (1959).

³⁴Q. Luo, B. Zhang, D. Q. Zhao, R. J. Wang, M. X. Pan, and W. H. Wang, *Appl. Phys. Lett.* **88**, 151915 (2006).

³⁵R. Busch, E. Bakke, and W. L. Johnson, *Acta Mater.* **46**, 4725 (1998); D. N. Perera, *J. Phys.: Condens. Matter* **11**, 3807 (1999).

³⁶T. Scopigno, G. Ruocco, F. Sette, and G. Monaco, *Science* **302**, 849 (2003).

³⁷D. Huang and G. B. McKenna, *J. Chem. Phys.* **114**, 5621 (2001).

³⁸M. A. Ramos, C. Talon, R. J. Jimenez-Rioboo, and S. Vieira, *J. Phys.: Condens. Matter* **15**, S1007 (2003).

³⁹L. M. Martinez and C. A. Angell, *Nature (London)* **410**, 663 (2001). Because the excess entropy of SiO₂ at T_g is puzzlingly small and the thermodynamic m related to the changes in the density of states in the vicinity of the BP, the kinetic m of SiO₂ is not connected to its thermodynamic m , and then induces the anomaly in this correlation.

⁴⁰H. Beck and H. J. Guntherodt, *Glassy Metals II* (Springer-Verlag, Berlin, 1983), Chap. 6.

⁴¹E. Leutheusser, *Phys. Rev. A* **29**, 2765 (1984).

⁴²G. H. Fredrickson and S. A. Brawer, *J. Chem. Phys.* **84**, 3351 (1986).

⁴³P. Wen, M. B. Tang, M. X. Pan, D. Q. Zhao, Z. Zhang, and W. H. Wang, *Phys. Rev. B* **67**, 212201 (2003).

⁴⁴M. Foret, E. Courtens, R. Vacher, and J. B. Suck, *Phys. Rev. Lett.* **77**, 3831 (1996).

⁴⁵V. Keppens, D. Mandrus, B. C. Sales, B. C. Chakoumakos, P. Dai, R. Coldea, M. B. Maple, D. A. Gajewski, E. J. Freeman, and S. Bennington, *Nature (London)* **395**, 876 (1998).

⁴⁶R. P. Hermann, R. Jin, W. Schweika, F. Grandjean, D. Mandrus, B. C. Sales, and G. J. Long, *Phys. Rev. Lett.* **90**, 135505 (2003).

⁴⁷A. Meyer, J. Wuttke, W. Petry, A. Peker, R. Bormann, G. Coddens, L. Kranich, O. G. Randl, and H. Schober, *Phys. Rev. B* **53**, 12107 (1996).

⁴⁸V. K. Malinovsky, V. N. Novikov, P. P. Parshin, A. P. Sokolov, and M. G. Zemlyanov, *Europhys. Lett.* **11**, 43 (1990).

⁴⁹Z. Zhou, C. Uher, D. Xu, W. L. Johnson, W. Gannon, and M. C. Aronson, *Appl. Phys. Lett.* **89**, 031924 (2006).

⁵⁰V. Keppens, Z. Zhang, O. N. Senkov, and D. B. Miracle, *Philos. Mag.* **87**, 503 (2007).

⁵¹D. B. Miracle, *Nat. Mater.* **3**, 697 (2004).

⁵²V. N. Novikov and A. P. Sokolov, *Phys. Rev. B* **74**, 064203 (2006); and references therein.

⁵³V. N. Novikov and A. P. Sokolov, *Nature (London)* **431**, 961 (2004); A. P. Sokolov, R. Calemczuk, B. Salce, A. Kisliuk, D. Quitmann, and E. Duval, *Phys. Rev. Lett.* **78**, 2405 (1997); D.-M. Zhu and H. Chen, *J. Non-Cryst. Solids* **224**, 97 (1998); and references therein.